Control of an AMB to Zero Static Force

Michael CAPLE[*], Eric MASLEN[**], Jacquelyn NAGEL[*] and Jacob WILD[*]

[*] Dept. of Engineering, James Madison University

801 Carrier Drive, Harrisonburg, Virginia 22807, United States

[**] Dept. of Integrated Science and Technology, James Madison University

701 Carrier Drive, Harrisonburg, Virginia 22807, United States

E-mail: masleneh@jmu.edu

Abstract

Some active magnetic bearing (AMB) applications require that the mean, or static force exerted by the AMB is zero. Examples include hybrid fluid film – AMB bearing pairings, rotor midspan dampers, and statically indeterminant systems with stiff rotors and more than two radial AMBs. When the position of the rotor relative to magnetic center is not known precisely, this zero force requirement can be hard to meet. A low frequency periodic biasing scheme is developed which enables a controller to detect non-zero static force by sensing rotor motion at the bias carrier frequency. A theoretical basis establishes feasibility but also the potential for coupling between control signals and the periodic bias. Simulation demonstrates that an ad–hoc bias adaptation scheme can successfully drive the static component to zero while permitting otherwise conventional control. The simulation results also show some spurious harmonic content associated with the sum and difference between a control signal frequency and the bias carrier frequency. Experimental results on a small, single DOF test rig further demonstrate the ability to drive the AMB static force to zero while adding damping to the system.

Key words : periodic control, biasing, AMB damper, zero static force, bias linearization

1. Introduction

In general, it is difficult to know the actual static force applied by an active magnetic bearing (AMB) because of uncertainty in shaft position relative to the magnetic center of the AMB. In many applications, this is not a problem because the AMBs are meant to carry the static loads applied to the rotor and the number of AMBs is such that this support is statically determinate. So if the rotor is properly controlled, it is obvious that the AMBs are providing the correct static load and it may also be possible to estimate this load with high confidence. However, some applications of active magnetic bearings require load sharing between the AMB and an adjacent mechanical bearing (Dimitri et al., 2014). In such combination structures, it may be very difficult to ensure that the two adjacent bearings are not applying large opposing forces at zero frequency which produce no net force on the rotor but use up bearing load capacity – the load sharing problem. In other applications, such as magnetic dampers (Kasarda et al., 1989), a specific objective of the control is to ensure zero static force and this may be important either to avoid unintended rotor stress or to conserve AMB load capacity. In yet other applications, more than two AMBs may be applied to a relatively rigid rotor and, as with the mechanical load sharing problem, there is potential for un-constructive competition amongst the bearings (Knospe et al., 1997). A common feature of all of these applications is that, if any one AMB in the system were to be turned off, the rotor would achieve some specific and acceptable equilibrium. The goal of the present work is to estimate the static force response of each AMB in a system and, more specifically, to drive this static force to zero so that, even with the AMB turned on, the non-AMB equilibrium position is preserved.

2. Background

Most active magnetic bearings employ some form of bias linearization. This means that opposing magnetic sectors have currents controlled according to a rule similar to

$$I_{x,1} = I_b + i_c(t) \qquad I_{x,2} = I_b - i_c(t) \tag{1}$$

in which I_b is some constant bias current and i_c is a symmetric perturbation applied to realize the bearing force (Schweitzer 2009). The subscript x refers to a direction of force application and the subscripts 1 and 2 denote the two opposing magnetic sectors. In the simplest approximation, the resulting behavior of the bearing is described by

$$f_x(t) = f_{x,0}(I_b, x_0) + k_x(I_b, x_0)(x(t) - x_0) + k_i(I_b, x_0)i_c(t) \tag{2}$$

Here, $f_{x,0}$ is the static force while coefficients k_x and k_i are the open-loop or magnetic stiffness of the sector pair and the actuator gain, respectively. All three are, as shown here, implicitly functions not only of the bias current, I_b, but also of the equilibrium rotor position, x_0. Even with the very best characterization of these terms, fundamental uncertainty in x_0 can lead to substantial uncertainty in the average value of f_x. In the classes of application considered here, this static position under which the static bearing force should be zero can change with time and machine operating conditions, so there is a need to be able to continuously monitor and regulate the static force.

Fundamentally, this uncertainty in static force is created by uncertainty in the rotor position relative to the magnet array effective magnetic center – the rotor position where equal currents in all coils leads to no net force. In AMBs with conventional bias, offset of the rotor position leads in an obvious way to a static force equal to the position offset times the negative magnetic stiffness associated with the biasing. AMBs with no bias that are able to adequately function activating only one of a pair of opposing coils at a time are still susceptible to an uncertain static force. This can be seen by assuming

$$f = \lambda_1 i_1^2 - \lambda_2 i_2^2 \tag{3}$$

in which rotor offset from magnetic center leads to $\lambda_1 \neq \lambda_2$. For such a bearing, if we assume for the sake of argument that the two currents can approximate

$$i_1 = \sqrt{\max(0, A\sin\omega t)} \qquad i_2 = \sqrt{\max(0, -A\sin\omega t)} \tag{4}$$

then the force history is

$$f(t) = \lambda_1 \max(0, A\sin\omega t) - \lambda_2 \max(0, -A\sin\omega t) \tag{5}$$

If $\lambda_1 = \lambda_2 = \lambda$ then the force is just $f(t) = \lambda A \sin\omega t$. But if $\lambda_1 \neq \lambda_2$, then the average force may be computed to be

$$\bar{f} = \frac{\omega}{2\pi}\int_0^{2\pi/\omega} [\lambda_1 \max(0, A\sin\omega t) - \lambda_2 \max(0, -A\sin\omega t)]\,dt = \frac{A}{\pi}(\lambda_1 - \lambda_2) \neq 0 \tag{6}$$

Thus, even absent a static biasing scheme, rotor offset relative to magnetic center leads to a non–zero static force.

3. Approach

To get around the problem of uncertain static load with uncertain rotor–magnetic center misalignment, consider the consequences of using a bias which is a combination of constant and periodic (sinusoidal) terms:

$$I_{x,1}(t) = (1+\beta)\left(I_{b,0} + I_{b,s}\sin\omega_b t + i_p(t)\right) \qquad I_{x,2}(t) = (1-\beta)\left(I_{b,0} + I_{b,s}\sin\omega_b t - i_p(t)\right) \tag{7}$$

Here, the nominal constant bias is $I_{b,0}$ but a periodic component with amplitude $I_{b,s}$ and frequency ω_b is added. The relative magnitudes of these persistent biases are not equal between the two sectors: β defines the relative magnitude. As before, active control will be accomplished by manipulating the now–potentially asymmetric perturbation current, $(1 \pm \beta)i_p(t)$. Further, assume that the position of the rotor relative to the magnetic center may be described by knowing the effective air gap lengths, g_1 and g_2, associated with the two opposing sectors so that without loss of generality,

$$g_1 = g_0(1+\gamma) \qquad \text{and} \qquad g_2 = g_0(1-\gamma) \tag{8}$$

in which the instantaneous journal position relative to magnetic center is $x = g_0\gamma$. Obviously, uncertainty in nominal position x_0 translates to corresponding uncertainty in γ.

With these assumptions, we can compute the force generated by an opposed pair of magnets:

$$\begin{aligned} f_x(t) &= \lambda\left(\frac{I_1^2}{g_1^2} - \frac{I_2^2}{g_2^2}\right) = \lambda\frac{(1+\beta)^2\left(I_{b,0} + I_{b,s}\sin\omega_b t + i_p(t)\right)^2}{g_0^2(1+\gamma(t))^2} - \lambda\frac{(1-\beta)^2\left(I_{b,0} + I_{b,s}\sin\omega_b t - i_p(t)\right)^2}{g_0^2(1-\gamma(t))^2} \\ &= \frac{4\lambda}{g_0^2(1-\gamma^2)^2}\left((1-\gamma\beta)(\beta-\gamma)(i_b^2 + i_p^2) + (1+\beta^2 - 4\gamma\beta + \gamma^2 + \beta^2\gamma^2)i_b i_p\right) \end{aligned} \tag{9}$$

in which λ is a magnetic constant that depends on pole area and coil turns and $i_b(t) \equiv I_{b,0} + I_{b,s} \sin \omega_b t$. In the case that $i_p = 0$, it is clear that the force goes to zero when $\beta \to \gamma$. Further, if it is possible to achieve $\beta = \gamma$ then

$$f(\beta = \gamma) = \frac{4\lambda}{g_0^2} i_b(t) i_p(t) \tag{10}$$

Define an alternate control variable $i_c(t)$ through

$$i_p(t) = \frac{I_{b,0}}{i_b(t)} i_c(t) = \frac{I_{b,0}}{I_{b,0} + I_{b,s} \sin \omega_b t} i_c(t) \tag{11}$$

to produce

$$f(\beta = \gamma) = \frac{4\lambda I_{b,0}}{g_0^2} i_c(t) \tag{12}$$

so that the signal to force relationship $i_c \to f$ is linear and time invariant. Note that, as long as $I_{b,s} < I_{b,0}$, then the inverse required by Eq. (11) always exists and only depends on known parameters.

The value of this result is that, if $i_c(t)$ has no components at zero frequency or at ω_b, then any force applied by the AMB at zero frequency will be matched by a component at a frequency of ω_b with a proportional magnitude. With this, the control strategy to achieve zero static force is to detect rotor response at ω_b using a fixed frequency high–Q filter and drive this response to zero by choice of β. Because the response at ω_b (i.e.: the signed Fourier response component) is monotonic in β, the control process is a simple search on β. Beyond this, the remainder of control of the AMB is as with any conventional AMB: the force is linear in $i_c(t)$ so conventional control algorithms will work as expected with the caveat that they must be conditioned to have a zero average value and to avoid the frequency ω_b.

In the present work, the heuristically justified control for β starts by generating the convolution signal $c(t)$:

$$c(t) = \int_{t-T}^{t} (x(\tau) + x_0) \sin \omega_b \tau \, d\tau \qquad : \qquad T = \frac{2N\pi}{\omega_b} \tag{13}$$

in which N is some positive integer on the order of 5. With this signal in hand, evolution of β is controlled by

$$\beta(t) = \int_0^t K_\beta c(\tau) \, d\tau \tag{14}$$

Here, the coefficient K_β is a tunable control parameter. Given the highly nonlinear nature of this problem, proof of convergence of $\beta \to \gamma$ is non–trivial and beyond the scope of the present work but, as will be illustrated in the sequel, this control is sufficient for at least some range of the system parameters.

Of course, this time–invariant linearization assumes that it is actually possible to ensure that $\beta = \gamma$ but since γ reflects the rotor position and is therefore time varying, it is prudent to assume that this is only an approximation and will affect the actual performance achieved. In light of this limitation, the ensuing simulations and experimental investigation will explore the consequences of this inevitable coupling.

4. Simulation

The first simulation explores the control of β. In this simulation, the choice is made that $i_p(t) = 0$ so the only objective is to ensure that the AMB applies no force to the rotor even though it is biased (gap fluxes are not zero) and the rotor is not located at the magnetic center. Of course, in the simulation, the control mechanism for achieving $\beta = \gamma$ has no intrinsic knowledge of γ but, rather, only sees the output of a convolution of x with $\sin \omega_b t$: $c(t)$ as defined by Eq. (13). Lacking conventional feedback control, this process is only stable as long as there is something in the mechanical structure to counteract the destabilizing influence of what is ordinarily referred to as the magnetic stiffness, or K_x. The present simulation considers a mass, $m = 0.5$ kg, connected to a spring $K_m = 3$ kN/mm and damper $C = 7.75$ N-sec/mm, where the spring is offset to give an equilibrium position other than magnetic center: this is illustrated in Fig. 1. The nominal bias is $I_{b,0}$ is 2.6 amps and the periodic bias is at 5 Hz with amplitude $I_{b,s} = 0.26$ amps. The nominal air gap is 0.5 mm and the spring equilibrium offset is 0.115 mm relative to magnetic center. The magnetic stiffness at the mechanical equilibrium position is $K_x = -1.34$ kN/mm so it is a little more than 1/3 of the mechanical stiffness.

The results are illustrated in Fig. 2. Control of β first turns on at $t = 1.2$ seconds and it is seen that the value of β rises to a peak at about 3.3 seconds before settling in to a very accurate estimate of the equilibrium value of $\gamma = 0.23$. Although the coil currents are persistent and substantial on both sides, the net magnetic force and associated mechanical force both go to zero as desired.

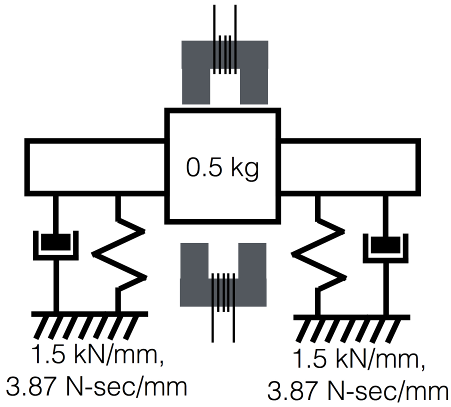

Figure 1: Mechanical model for the simulation. Notice that the spring equilibrium position does not coincide with the magnetic center of the opposed electromagnets.

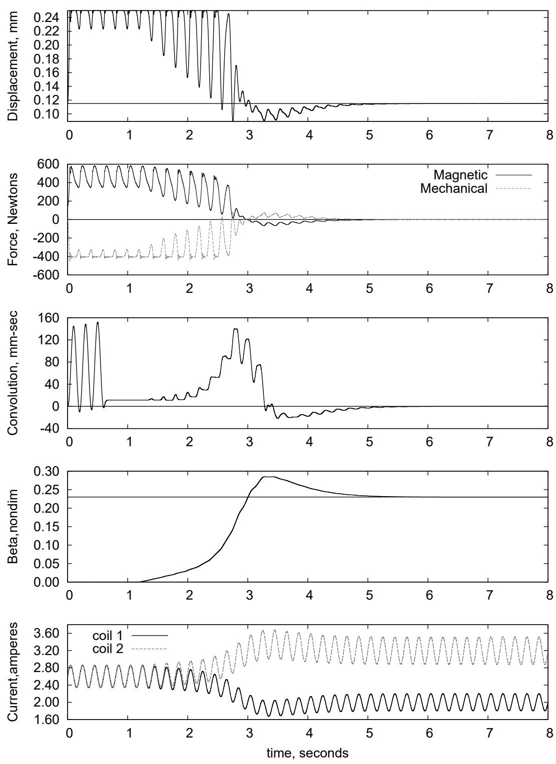

Figure 2: Simulation results with only bias rebalancing control.

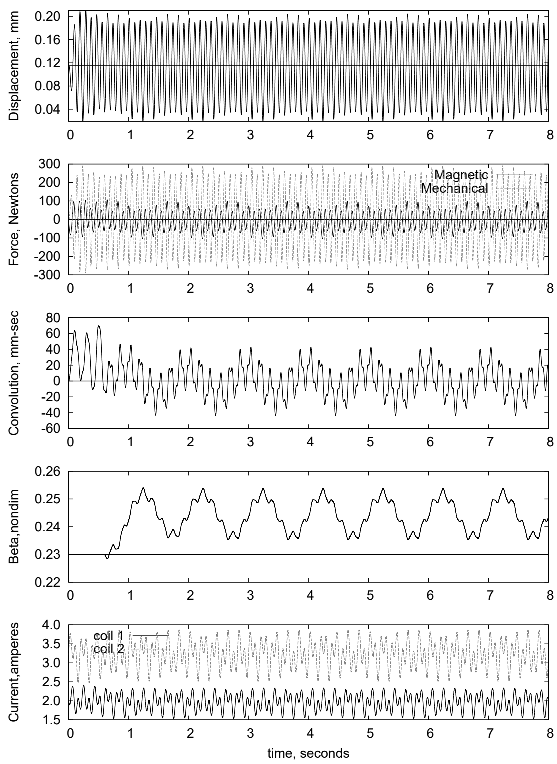

Figure 3: Simulation results with bias rebalancing and active control at 11 Hz. β was initialized at its steady state value.

The second simulation explores the effectiveness of the control signal, $i_p(t)$. In this simulation, β is initialized at a value leading to equilibrium with $i_p = 0$. A sinusoidal signal is then injected so that $i_p(t) = a \sin \omega t$ with ω chosen to be other than the periodic bias frequency of 5 Hz. A typical example is illustrated in Fig. 3 which illustrates the response at 11 Hz. First, it is clear that the rotor motion tracks the 11 Hz control signal. This is especially evident in the response spectrum presented in Fig. 4 which shows a substantial peak at 11 Hz. Beyond this, it is evident that there is some response

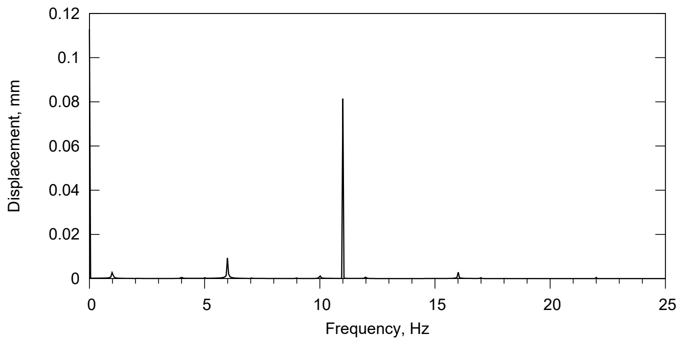

Figure 4: Spectrum of mass displacement with both bias rebalancing and active control at 11 Hz.

at the sum and difference between the target frequency and the carrier: the peaks at 6 Hz and at 16 Hz. Presumably, these are consequences of coupling that arises because the β−adaptation is not perfect and is not able to perfectly maintain $\beta = \gamma$ when the rotor is moving. That said, the responses at off–frequencies are quite small relative to the intended response so this coupling may be acceptable in practical use.

5. Experimental Demonstration

To demonstrate this control strategy, a very simple single–DOF magnetic bearing based on a very simple magnetically actuated rocking beam apparatus (Knospe, 2000) is modified by adding a spring between the rocking beam and ground as illustrated in Fig. 5. The goal is to control the AMB in such a way that, regardless of the pre-load position of the spring,

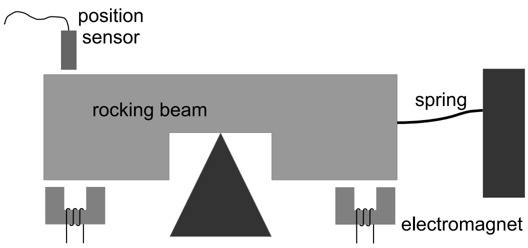

Figure 5: Rocking beam apparatus with electromagnets and preloaded spring.

the AMB will not deflect the spring. This may sound simple, but quick analysis and simple experiments will reveal that, unless it is possible to actually measure the spring deflection (not the same as measuring beam position), it is not possible to control a conventional AMB to ensure that this deflection is actually zero. The feedback control implemented is a simple damping mechanism and the experiments show that the resulting level of damping can be controlled in a predictable manner while ensuring that the static AMB force (indicated by spring strain) stays zero for any spring preload position.

Figure 6 shows convergence of the bias balance adaptation. At $t = 0$, the rotor is in its mechanical equilibrium position with the AMB turned off. The AMB is turned on with β initialized to zero and the data show the adaptation process as β approaches 0.141 as well as the recovery of rotor position to its mechanical equilibrium as indicated by the convolution signal going to zero.

Figures 7 through 10 illustrate the impact response of the system with various kinds of AMB control. In each case, the rocker mass is struck with a plastic mallet and the resulting motion recorded. In Fig. 7, the AMB is inactive so the rocker mass and the spring control the dynamics. There is some structural damping, but it is light so the oscillation decays slowly. In Fig. 8, the AMB is active (periodic bias is activated) but its control is configured to do nothing. What

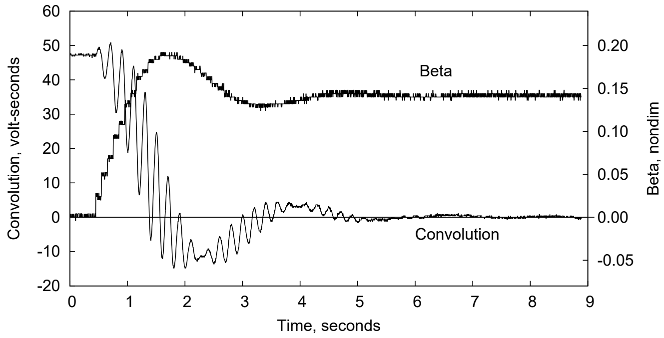

Figure 6: Experimental demonstration of bias balance adaptation. The adaptation process only has access to the convolution of the position sensor signal with the reference sine wave so it does not know what the equilibrium value of position or of β should be. Convergence is achieved when the convolution signal goes to zero, indicating no rocker response at the bias frequency of 5 Hz.

is apparent is that the response to the mallet hit is essentially the same as with the AMB turned off. That is, the static position has not changed nor has the damping or natural frequency appreciably changed. In Fig. 9, the AMB is active and its control is designed to generate damping ($K_d s/(\tau s + 1)$). The damping coefficient is set to a moderate level of 0.01 units with $\tau = 0.001$ seconds and the response is seen to be much more heavily damped than without the AMB but to exhibit some oscillation after the impulse. In Fig. 10, the AMB is again active with damping control but here the damping coefficient has been increased by a factor of three to 0.03 units. The response now shows no appreciable oscillation, clearly demonstrating a heavily overdamped behavior.

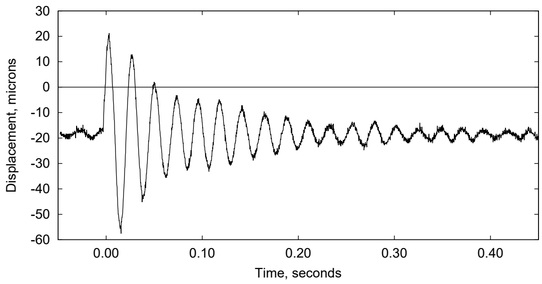

Figure 7: Experimental displacement response to a strike of a plastic mallet. The AMB is not active so damping is quite light.

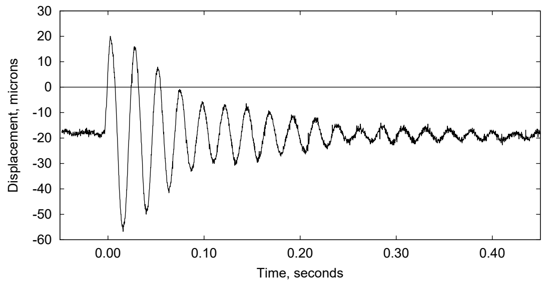

Figure 8: Experimental displacement response to a strike of a plastic mallet. The AMB is active but damping is set to zero: response is the same as with the AMB inactive.

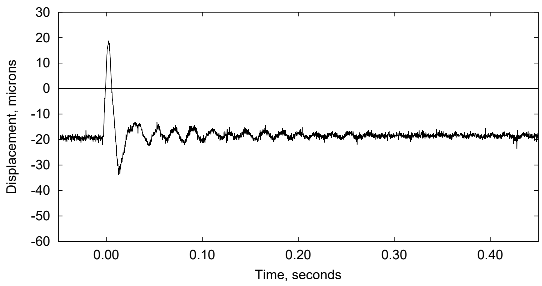

Figure 9: Experimental displacement response to a strike of a plastic mallet. The AMB is active and damping is moderate (0.01 units).

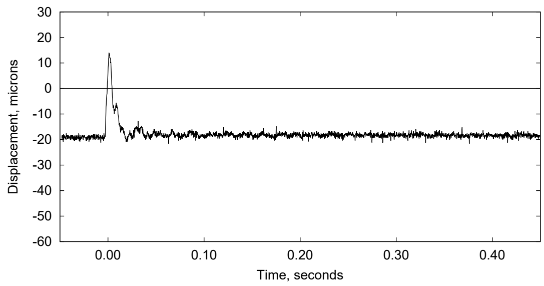

Figure 10: Experimental displacement response to a strike of a plastic mallet. The AMB is active and damping is high (0.03 units).

6. Conclusions

The work presented here clearly demonstrates a method to enable an AMB to adapt its bias distribution so as to produce no static force even when the static position of the rotor relative to the AMB magnetic center is unknown. The method exploits adding a low frequency periodic component to the biasing field and detecting rotor response at the same frequency to determine whether or not the AMB is exerting force at the carrier frequency and, by implication, a static force. The relative amplitude of bias in opposing quadrants of the AMB is then adjusted to bring the response at the carrier frequency to zero and this achieves the desired zero static force. Further, it is possible and reasonably simple to invert the periodic actuator gain induced by this periodic bias and the resulting AMB may be used in the same way that a conventionally biased AMB is used.

Simulation results point to some potential deficiencies of the approach in that there is some residual coupling between the carrier signal and the control signal which results in response at the sum and difference of frequencies. In some applications, this residual coupling could be problematic, especially if it led to unintended excitation of lightly damped structural modes. Clearly, this issue merits further investigation.

Application of this approach to practical rotating machinery will require, among other extensions, the ability to simultaneously adapt in two directions and potentially at multiple machine planes. It is assumed here that these multiple adaptation axes can be separated by using different carrier frequencies for each axis. Clearly, the carriers must be well enough separated to be readily distinguished with relatively short convolution windows: only a few cycles of each carrier. This will require substantial investigation beyond the hints provided in the present work, but does not appear to be insurmountable.

It is also important to note that the bias adaptation is only stable when the mechanical stiffness of the structure is substantially higher than the magnitude of the negative magnetic stiffness of the AMB. In the present study, it was found that a factor of about three was generally sufficient but further theoretical investigation might usefully provide a hard bound on this ratio and this would obviously affect the achievable size of the AMB in specific applications.

7. Acknowledgements

The authors would like to acknowledge the support of the US National Science Foundation (grant number IIA-1445804) which enabled this work. They would also like to acknowledge the very fruitful collaboration of Dr. Aly El Shafei and Dr. Antoine Dimitri of Cairo University.

References

Dimitri, A. S., Mahfoud, J., and El-Shafei, A., “Oil Whip Elimination Using Fuzzy Logic Controller,” Proc. ASME Turbo Expo, Dusseldorf, 2014.

Kasarda, M. E. F., et al. “A magnetic damper for first mode vibration reduction in multimass flexible rotors.” ASME 1989 International Gas Turbine and Aeroengine Congress and Exposition. American Society of Mechanical Engineers, 1989.

Knospe, Carl R., Roger L. Fittro, and L. Scott Stephens. “Control of a high speed machining spindle via/spl mu/-synthesis.” Control Applications, 1997., Proceedings of the 1997 IEEE International Conference on. IEEE, 1997.

Knospe, C.R., “The nonlinear control benchmark experiment,” in Proc. Amer. Control Conf., Chicago, IL, 2000, pp. 2134–2138.

Schweitzer, G. and Maslen, E. (ed.) *Magnetic Bearings Theory, Design, and Application to Rotating Machinery,* Springer, 2009.